 Journal of Polytechnic, 2017; 20 (1) : 25-36

A Parametric Study on the Heterogeneous Photo-Fenton-Like Oxidation of Bisphenol-A over an Fe/TiO_2 Catalyst under Visible Light

Meral DÜKKANCI

Ege University, Faculty of Engineering, Chemical Engineering Department, 35100, Bornova/Izmir/Turkey

(Received : 18.02.2016 ; Accepted : 03.05.2016)

ABSTRACT

In this study the oxidation of Bisphenol-A (BPA) was investigated using heterogeneous photo-Fenton-like oxidation under visible light irradiation over iron containing TiO_2 catalysts. The catalysts were prepared by the incipient wetness impregnation method with different iron contents (1 and 5 wt%) and characterized by XRD, SEM, FT-IR, nitrogen adsorption, UV-Vis DRS, and ICP-AES measurements. Among the prepared catalysts the 1 wt% iron containing the TiO_2 catalyst showed better catalytic activity (with a chemical oxygen demand (COD) reduction of 65.4% at the end of 6h of oxidation) than the other catalysts. The effects of the parameters such as the initial BPA concentration, H_2O_2 amount, catalyst amount, the pH of the initial BPA solution, and reaction temperature were studied with that catalyst on the heterogeneous photo-Fenton-like oxidation of an aqueous BPA solution. The small amount of iron that leached to the solution and the reusability of the catalyst illustrates that the process is mainly the heterogeneous photo-Fenton-like process, instead of the homogeneous photo-Fenton-like process. The degradation of BPA was described by the first order kinetics with an activation energy of 22.5 kJ/Mol.

Keywords: Photo-Fenton-like Oxidation, Bisphenol-A, Fe/TiO_2 Catalysts.

Bisfenol-A'nın Görünür Bölge Işığında ve Fe/TiO_2 Katalizörü üzerinde Heterojen Foto-Fenton-Tipi Oksidasyonu üzerine Parametrik Çalışma

ÖZ

Bu çalışmada Bisfenol-A'nın (BPA) demir içeren TiO_2 katalizörleri ve görünür bölge ışığı varlığında heterojen foto-Fenton-tipi oksidasyonu incelenmiştir. Bu bağlamda, öncelikle farklı demir miktarlarında (ağırlıkça %1 ve %5) ıslatarak emdirme yöntemiyle TiO_2 katalizörler hazırlanmış ve XRD, SEM, FTIR, Azot Adsorpsiyon, UV-Vis DRS ve ICP-AES teknikleri ile karakterize edilmiştir. En iyi aktivite gösteren ağırlıkça %1 demir içeren TiO_2 katalizörü ile BPA'nın heterojen foto-Fenton tipi oksidasyonunda 6 saat sonunda %65,4'lük COD (Kimyasal Oksijen İhtiyacı) giderimi elde edilmiştir. BPA'nın heterojen foto-Fenton-tipi oksidasyonuna, BPA başlangıç derişimi, H_2O_2 ve katalizör miktarları, BPA çözeltisinin başlangıç pH değeri ve reaksiyon sıcaklığının etkileri incelenmiştir. Çözeltiye özütlenen demir miktarının düşük olması ve katalizörün yeniden kullanılabilirliğinin yüksek olması, reaksiyonun homojen foto-Fenton-tipi oksidasyonundan ziyade heterojen foto-Fenton-tipi oksidasyonu olduğunu göstermektedir. Çalışmada BPA bozunma kinetiği de incelenmiş, bozunmanın birinci mertebeye uyduğu gözlenmiş ve aktivasyon enerjisi 22,5 kJ/Mol olarak hesaplanmıştır.

Anahtar Kelimeler: Foto-Fenton-Tipi Oksidasyon, Bisfenol-A, Fe/TiO_2 Katalizörler.

1. INTRODUCTION

Bisphenol-A (BPA) is an organic compound composed of two phenol rings connected to a poly group at the center carbon and has been widely accepted as one of the important monomers for the production of a variety of chemical materials such as polycarbonate, epoxy resins, and flame retardants. Due to an increase in the use of products based on epoxy resins and polycarbonate plastics, exposure of humans to BPA through several routes such as the environment and food has increased [1] and BPA has been frequently detected in both industrial wastewater and drinking water sources (in the range of 0.02 - 50 ppm). BPA is known as an endocrine-disrupting compound with its estrogenic activity and toxicity to human. BPA also may play a role in thyroid hormone dysfunctions, central nervous system function disorder, and immune suppression [2]. BPA also has an acute toxicity in the range of about 1-10 $\mu g/cm^3$ for a number of freshwater and marine species. Because of the above reasons, BPA must be removed from wastewater with suitable technologies. However, conventional processes for water treatment may be inefficient for the elimination of BPA totally. Therefore, several alternative processes have been proposed. Of all the methods developed so far, the Advanced Oxidation Processes (AOPs) offer several particular advantages in terms of

**Sorumlu Yazar (Corresponding Author)*
e-posta: meral.dukkancı@ege.edu.tr
Digital Object Identifier (DOI) : 10.2339/2017.20.1 25-36

unselective degradation of BPA into a final mineralized form with the production of highly oxidative hydroxyl radical ($OH^{\cdot}$) [3]. AOPs such as, sonication [1, 4-9], comparative oxidation of sonication and homogeneous Fenton reaction [10], sonoFenton reaction [11-13], photo-Fenton reaction [14], sorption on the goethite [15], photo oxidation [16, 17], photocatalytic degradation in the presence of TiO_2 catalysts [18-27], photocatalytic degradation in the presence of Al_2O_3-Fe_2O_3, Bi_2WO_6/$CoFe_2O_4$, Bi_2WO_6, $Bi_{3.84}W_{0.16}O_{6.24}$, and Ag_3PO_4 catalysts [28-32], photo-Fenton like oxidation over Au/C catalyst [33], ozone+UV oxidation [34], ozonation [35, 36], sonophotocatalytic oxidation [37, 38], homogeneous Fenton oxidation [39], oxidation over a $SrFeO_{3-\delta}$ perovskite catalyst in the dark [40], and H_2O_2-assisted photoelectrocatalytic oxidation [41] were used individually or in combination with each other to degrade BPA containing wastewater. C-N co-doped TiO_2, Bi_2WO_6, magnetic $BiOBr@SiO_2@Fe_3O_4$, a graphene-oxide/$AgPO_4$ composite, and a mesopolymer modified with palladium phthalocyaninesulfonate catalysts [30, 42-45] were used successfully in the photocatalytic degradation of BPA under visible light.

Among the used AOPs, the photocatalytic oxidation process has been the focus of numerous investigations in recent years. In this concern, TiO_2 has been extensively studied as a semiconductor photocatalyst because of its relatively high photocatalytic activity, chemical stability, low cost, and environmental friendliness. However TiO_2 is only active under UV light irradiation due to its large band gap energy (3.2 eV) which results in a low efficiency to make use of solar light [46, 47]. Whereas, ultraviolet light makes up only 4-5% of the solar spectrum, and approximately 40% of the solar photons are in the visible region. Therefore, in order to enhance the solar efficiency of TiO_2 under solar irradiation, significant efforts have been made in the past decades to develop TiO_2-based photocatalysts capable of using abundant visible light in solar radiation or artificial light. Many strategies, including the surface modification, metal ion (Ce, In, Ag, etc.) doping, nonmetal ion (N, C, S etc.) doping, coupling with other narrow band-gap semiconductors etc. have been adopted to synthesize TiO_2-based visible light activated photocatalysts. Metal ion doped TiO_2 has been widely studied due to not only the expanded spectral response but also the enhanced photocatalytic activity. Moreover, metal doping can improve the structure and morphology of a photocatalyst, decrease the probability of the charge carrier recombination, and promote the effective separation of the charge carrier. Among various dopants, the Fe^{3+}-dopant is the most frequently employed one, owing to its unique half-filled electronic configuration, which narrows the energy gap while inducing new intermediate energy levels[48]. The presence of the Fe^{3+} in the catalyst also acts as a Fenton like catalyst and helps the production of more hydroxyl radicals via reactions 1-4 [49].

$$Fe^{2+} + H_2O_2 \longrightarrow Fe^{3+} + {\bullet}OH + OH^- \quad (1)$$

Iron (III) can then react with hydrogen peroxide in the so-called Fenton-like reaction (equations 2 and 4)

$$Fe^{3+} + H_2O_2 \longrightarrow FeOOH^{2+} + H^+ \quad (2)$$

$$FeOOH^{2+} \rightleftharpoons HO_2{\bullet} + Fe\ (II) \quad (3)$$

$$Fe\ (III) + HO_2{\bullet} \longrightarrow Fe\ (II) + O_2 + H^+ \quad (4)$$

This study presents the preparation and characterization of Fe containing TiO_2 catalysts and tests on their photocatalytic activities in the oxidation of Bisphenol-A (BPA) by the heterogeneous photo-Fenton-like oxidation under visible light irradiation. To the best of our knowledge, this study is first on the heterogeneous photo-Fenton like oxidation of BPA over Fe containing a TiO_2 catalyst under visible light.

2. EXPERIMENTAL STUDY

2.1 Catalyst Preparation

Iron containing TiO_2 catalysts were prepared by the incipient wetness impregnation method used by Arana et al. [50] and Demir et al. [51]. An aqueous solution of Fe $(NO_3)_3.9H_2O$ (Sigma Aldrich) was added slowly to a proper amount of TiO_2 (Sigma Aldrich P-25, 80% anatase) and the mixture was stirred vigorously for 48 h. Then, the water of the mixture was evaporated by heating at 393 K for 24 h. The catalyst was then calcined at 773 K for 3 h. The catalyst has been denoted as TiO_2 for bare TiO_2 Sigma Aldrich P-25 and x Fe/TiO_2 for the doped one, where x is the Fe weight % (wt%) in the catalyst. The x was changed to be 1 and 5.

2.2 Experimental Procedure of the Heterogeneous Photo-Fenton-like Oxidation of BPA

Figure 1 shows the experimental set-up used for the heterogeneous photo-Fenton-like oxidation of BPA. In a typical experiment, 0.3 dm^3 of 15 ppm of BPA aqueous solution was poured into the cylindrical reactor and 0.5 g/dm^3 of catalyst was added to the solution and the suspension was left for 30 minutes in the dark to establish the adsorption-desorption equilibrium of the BPA on the catalyst surface. The amount of the BPA adsorbed by the catalyst was determined by measuring the BPA concentration after 30 min in the absence of visible light illumination. Then H_2O_2 was added and the visible light lamps were turned on. The solution was irradiated with two visible lamps (high pressure Na lamps, each 150 W). The heterogeneous photo-Fenton process for the degradation of BPA took 6 h. The reaction temperature was kept constant at 293±2K by circulating cooling water around the reactor to avoid the significant overheating of the reaction media. The reaction vessel was maintained in a box to avoid photochemical reactions induced by natural light. Experiments were performed at a BPA ambient pH which was about 5.5 and left uncontrolled during the experiments. Samples were periodically drawn from the vessel and centrifuged for 15 min and then analyzed with a UV spectrophotometer (Shimadzu, UV-Vis 1800). The decrease in the intensity of the band at 276 nm was used as a measure of degradation degree.

In addition to these measurements, the Chemical Oxygen Demand (COD) removal of the BPA solution was

determined by measuring initial COD and final COD (at the end of the run) of the BPA solution with a COD device (Lovibond Checkit Direct COD Vario).

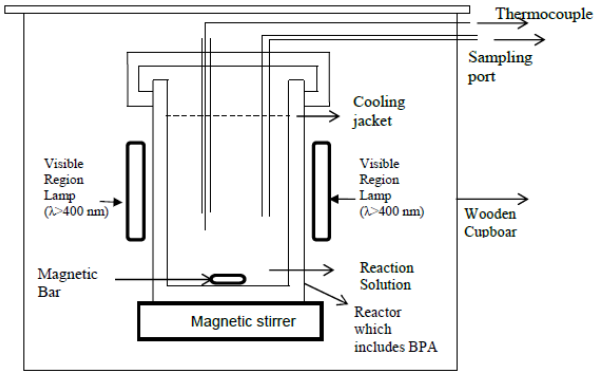

3. RESULTS AND DISCUSSION

3.1 Catalyst Characterization

The Powder X-ray diffraction (XRD) patterns of the catalysts were recorded in the range of 5-80˚ with a Philips X'Pert Pro with Cu-Kα radiation to determine the crystalline structure of the samples. The morphological properties were analyzed with a scanning electron microscopy (FEI Quanta250 FEG). The nitrogen adsorption isotherms at 77 K were measured using the Micromeritics ASAP 2010 equipment. The FT-IR spectra was recorded in the 650-3650 cm^{-1} with a Perkin Elmer Spectrum 100 spectrometer. The content of iron in the samples was determined by a Varian-96 Inductively Coupled Plasma Atomic Emission Spectrometer (ICP-AES). The band gap energy value measurements were accomplished using a UV-Vis DRS /Shimadzu 2600.

According to the XRD patterns of the catalyst samples (Figure 2), the samples have both anatase and rutile phases. The peaks at 2θ = 25.4°, 37.9°, 48.1°, 53.9 °, 55.2°, and 62.9° are attributed to the diffractions of the anatase phase and the peaks at 2θ = 27.5°, 36.0°, and 41.2° to the rutile phase [51, 52].

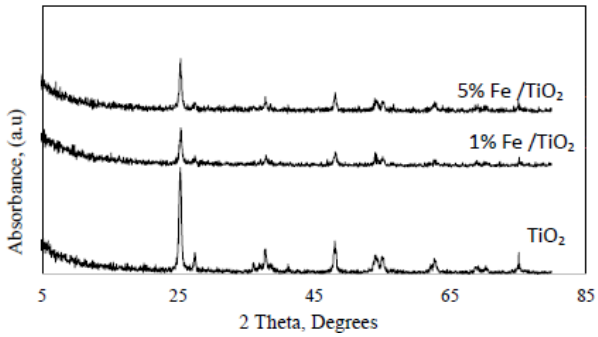

Figure 2. XRD patterns of the prepared catalysts

In the FTIR spectra of the prepared catalysts, there was a broad band at the range of 3150 - 3650 cm^{-1} which is assigned to the Ti-OH stretching band [51, 53]. The intensity of this band decreases with the insertion of Fe into the structure. The band at 1640 cm^{-1} indicates the deformation vibration that is evidence for a large amount of water molecules.

The morphological properties were analyzed using a scanning electron microscopy, Figure 3. The surface of the TiO_2 sample without iron looked coral-like. Heavily aggregated particles of very small crystallites were observed. There is no significant difference between the SEM images of the TiO_2 and the 1 wt% Fe containing TiO_2 sample. However, the insertion of a high amount of iron (5%) into the TiO_2 separated the aggregates of TiO_2 particles from each other which caused a slight decrease in the pore volume and the surface area of the sample [51, 52, and 54]

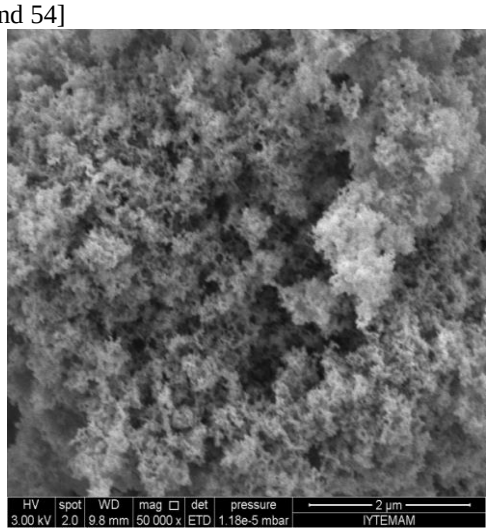

a)

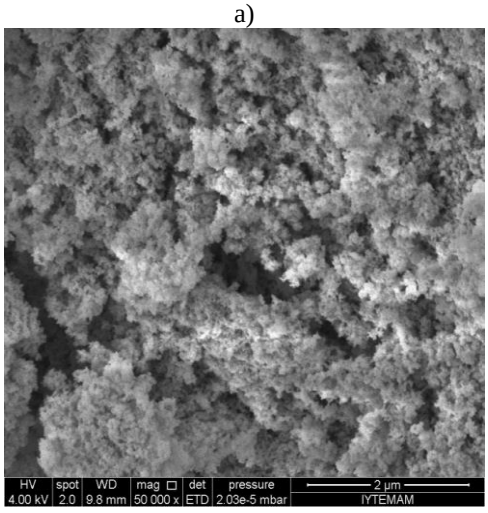

b)

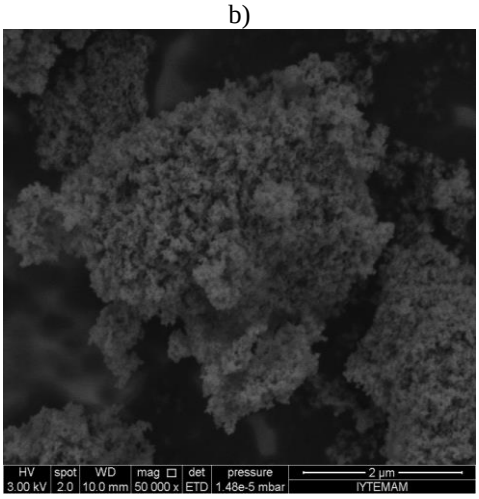

c)

Figure 3. SEM images of the samples

a)TiO_2 **b)**1% Fe/TiO_2 **c)** 5% Fe/TiO_2

The BET-surface area (S_{BET}), external surface area ($S_{external}$), total pore volume (V_p), and mean pore diameter (d_{mean}) obtained from the nitrogen adsorption/desorption measurements are shown in Table 1.

Table 1 shows that an increase in the Fe content led to a slight increase in the BET surface area of the catalyst. The pure TiO_2 surface area was 54.1 m^2/g and after the incorporation of 1wt % Fe the surface area increased to 55.5 m^2/g. The increase in the surface area with the introduction of the initial amount of Fe can be, generally, explained in two ways: as a result of the reorganization of the pore system of the starting material through the entrance of small particles into the pore system, or as a result of the deposition of the Fe species on the outer side of the TiO_2 particles. The reorganization of the initial system of pores must lead to a decrease of the total pore volume. However, there was no reduction in the total pore volume of the 1 wt% Fe containing TiO_2 catalyst. Clearly, the Fe species are dominantly located on the outer surface of the catalyst. The insertion of Fe to the TiO_2 also caused an increase in the external surface area of the catalysts where the photocatalytic degradation took place. A slight decrease in the surface area was observed with an increase in the doping level of Fe at a calcination temperature of 773 K [49, 51, 55].

The nitrogen adsorption isotherms of the samples are of type II according to IUPAC classification. This result is in good agreement with the study done by Wang et al. [56].

The content of iron in the samples was determined with ICP-AES measurements. The results are shown in Table 1. As seen, the calculated iron contents are very close to the ones measured with ICP-AES measurements.

3.1.1 Diffuse reflectance spectra of prepared catalysts

A modified Kubelka-Munk function was used for determining the band gap energy (E_g) of the TiO_2 and Fe-doped TiO_2 samples from the diffuse reflectance spectra, Eq.5:

$$(F(R)*h\nu)^{1/n}=B(h\nu-E_g) \quad (5)$$

Where h is Planck's constant, ν is the light frequency, B is a constant, $F(R) = (1-R)^2/2R$, R is reflectance, and $h\nu = (1240/\lambda)$ eV. The band gap can be classified as direct or indirect. In a direct band gap the energy minimum (the bottom) of the conduction band lies directly above the energy maximum (the top) of the valence band in reciprocal k-space. But in the indirect band gap, the energy minimum (the bottom) of the conduction band is away from the energy maximum (the top) of the valence band [57]. Values of n can be different depending on the type of electronic transition where n=2 for an indirect allowed transition and n=1/2 for a direct allowed transition. It has been suggested that anatase TiO_2 follows an indirect transition [58, 59] thus n=2 is used in this study. Figure 4 plots the $(F(R)*h\nu)^{1/n}$ versus the hν curve. The value of the band gap energy (E_g) can be obtained by extrapolating the linear part of the curve to the horizontal axis (hν axis). The indirect type transition showed band gap values of 3.05, 2.9, and 2.5 eV for catalysts TiO_2, 1% Fe/TiO_2, and 5% Fe/TiO_2, respectively. It was seen that the band gap decreases with increasing Fe content. Based on the band gap energies of the catalysts, the TiO_2 catalyst is expected to be active under UV irradiation, whereas, the Fe doped TiO_2 (with 1 wt% and 5 wt%) catalysts is expected to be active under visible light [59, 60].

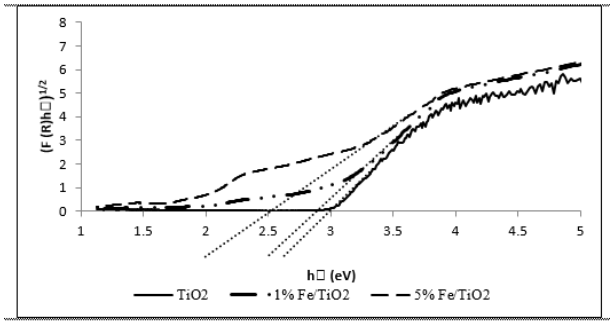

Figure 4. Diffuse reflectance spectra of the TiO_2 catalysts

Table 1. The BET-surface area (S_{BET}), External surface area ($S_{external}$), total pore volume (V_p), mean pore diameter (d_{mean}), and iron contents of the catalysts prepared

Catalysts	Fe, wt %	S_{BET}, (m^2/g)	$S_{external}$, (m^2/g)	d_{mean}*,nm	V_p,(cm^3/g)
TiO_2	0	54.1	45.9	5.91	0.01400
1% Fe/TiO_2	0.93	55.5	53.7	8.64	0.01500
5% Fe/TiO_2	4.46	50.5	47.3	8.85	0.01388

* by BJH method

3.2 Photo-Fenton-like Oxidation of BPA over Prepared Catalysts

3.2.1 Effects of catalyst type

The activity of the prepared catalysts with different iron contents (1 and 5 wt%) and bare TiO_2 were tested in the photo-Fenton-like oxidation of BPA under visible light. The experiments were carried out with a 15 ppm, 0.3 dm^3 BPA aqueous solution in the presence of a 0.5 g/dm^3 catalyst and 4.7 mM H_2O_2 at a temperature of 19±1°C. The results are shown in Figure 5.

A first order dependency was obtained in the photo-Fenton-like oxidation of BPA with a high regression coefficient in all the runs. The degradation rate constant of $k = 8.7x10^{-4}$ min^{-1} ($R^2 = 0.95$) was obtained for 1%

Fe/TiO_2, and $k = 6.7x10^{-4}$ min^{-1} ($R^2 = 0.97$) was obtained for 5% Fe/TiO_2.

As seen in Figure 5, the degradation of 24%, 21%, and 0.8% were obtained in the presence of 1 wt%, 5 wt% Fe containing TiO_2 catalysts, and bare TiO_2, respectively,

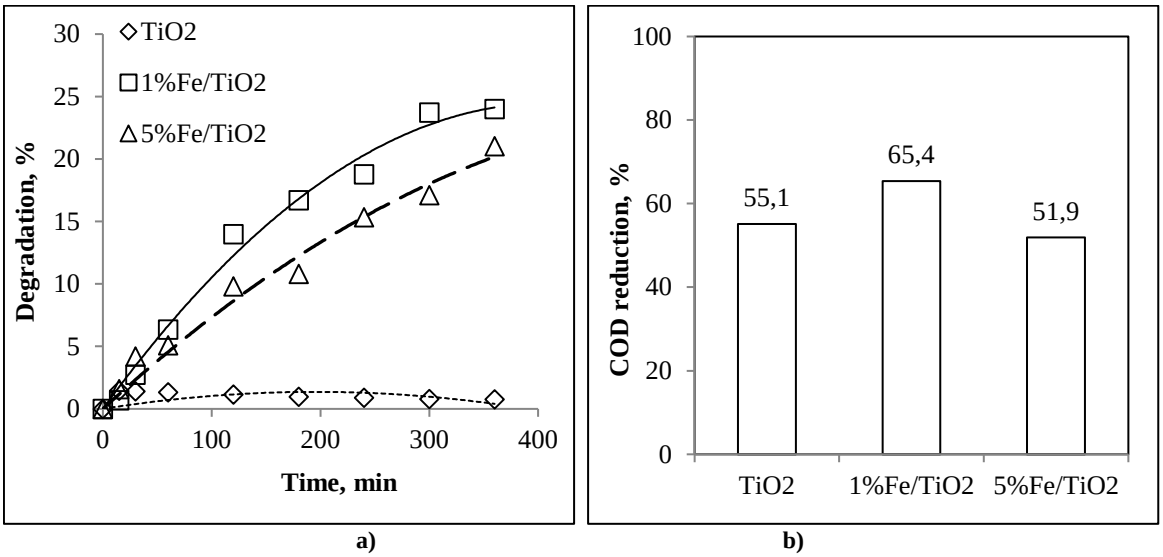

Figure 5. Effects of catalyst type on the photo-Fenton-like oxidation of BPA, **a)** Degradation, % and **b)** COD reduction, %, after 6 h of oxidation

after a reaction duration of 6 h. The corresponding COD reductions were 65.4%, 51.9%, and 55.1%. As seen, the most active catalyst was 1 wt% Fe containing TiO_2 catalyst in terms of the degradation and degradation rate constant as well as the COD reduction. The existence of a high amount of Fe (5 wt%) lessens the specific surface area of the TiO_2 and prevents the adsorption of the reactant and thus, inhibits the photocatalytic activity. An excess amount of dopant at the surface of the TiO_2 could notably screen off the TiO_2 from the light and inhibit the interfacial electron and hole to transfer, which would result in a low photo-activity [61]. So the parametric study on degradation of BPA with the heterogeneous photo-Fenton–like oxidation was carried out using the 1 wt % Fe containing TiO_2 catalyst.

3.2.1 Effects of the initial concentration of BPA

The effect of the initial BPA concentration on the BPA degradation was investigated using different initial BPA concentrations (5 ppm, 10 ppm, 15 ppm, and 20 ppm). The experiments were carried out with a 0.5 g/ dm^3 1 wt% Fe/TiO_2 catalyst, at 4.7 mM of H_2O_2 concentration at a temperature of 20±1°C and with a solution volume of 0.3 dm^3, the results are shown in Figure 6.

As shown in Figure 6, the highest BPA degradation was reached when the BPA initial concentration was 5 ppm (61.3%). The degradation of BPA decreased as the initial BPA concentration increased from 5 ppm to 20 ppm. The COD reduction also decreased remarkably from 85.9% to 50.4%. This result can be explained by the formation of the hydroxyl radicals which are less than the required amount for high BPA concentrations. As seen in Figure 6a, there is a remarkable decrease in the reaction rate constant with an increasing BPA concentration from 5 ppm to 20 ppm. This similar result is consistent with the study of Lu et al. [62].

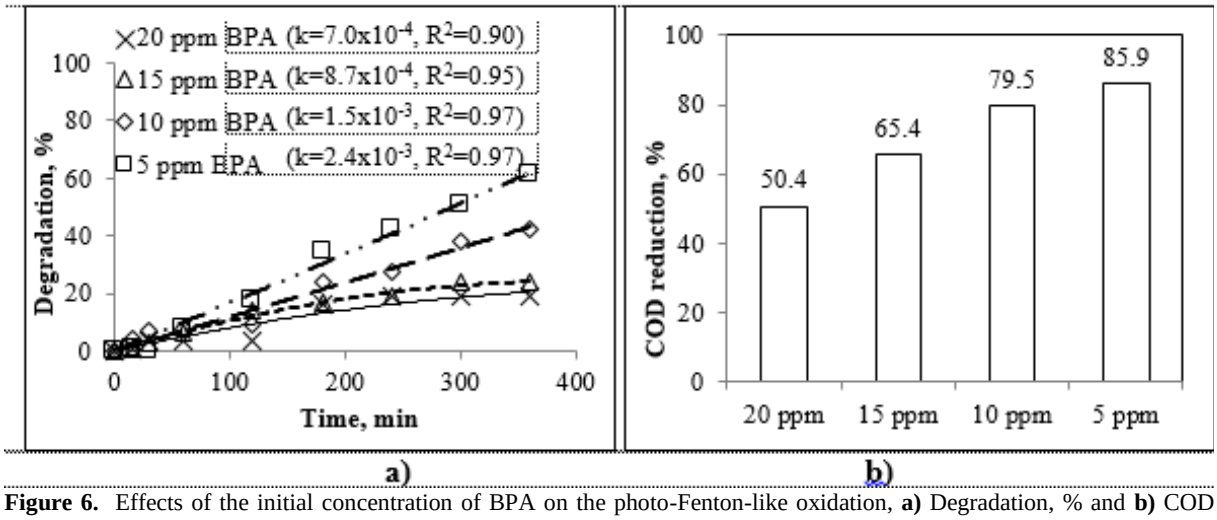

Figure 6. Effects of the initial concentration of BPA on the photo-Fenton-like oxidation, **a)** Degradation, % and **b)** COD reduction, %, after 6 h of oxidation

The active sites for the photocatalytic reaction remain the same at a fixed catalyst amount. As the BPA initial concentration increases, more and more BPA molecules are adsorbed on the surface of the catalyst. The accumulation of BPA molecules in the inner layer spacing on the TiO_2 surface results in the adsorption competition for the active sites between the BPA molecules and the prevention of the photocatalytic

The increase in degradation may be expected when the H_2O_2 concentration is increased due to the additionally produced ·OH radicals [32]. In this study, the highest degradation (52.0%), reaction rate constant ($k=1.8x10^{-3}$ min^{-1}), and COD reduction of BPA (72.3%) were observed when H_2O_2 was used at 1.5 times that of the stoichiometric ratio (3.6 mM), see Figures 7a-b. Increasing the H_2O_2 concentration did not enhance the

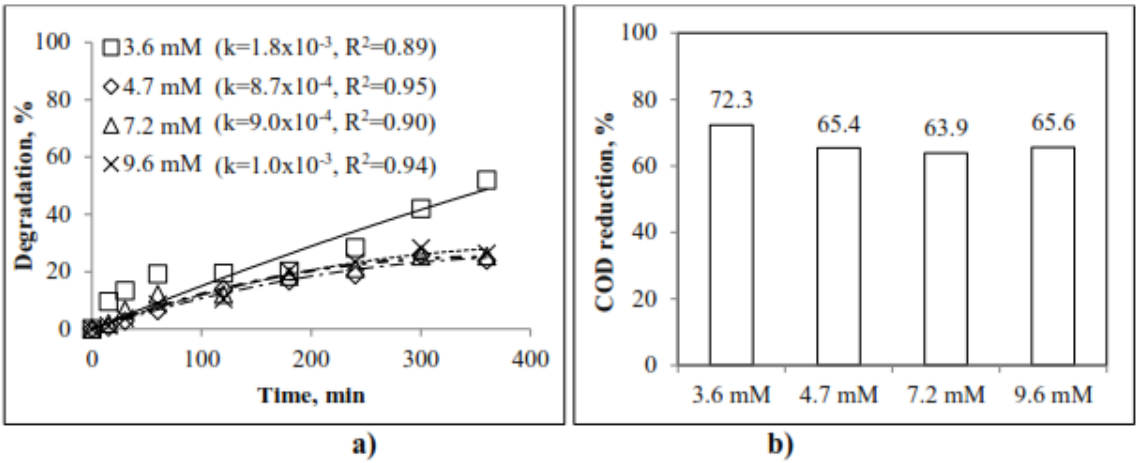

Figure 7. Effects of the initial concentration of H_2O_2 on the photo-Fenton-like oxidation, **a)** Degradation, %, and **b)** COD reduction, %, after 6 h of oxidation

activity of the TiO_2 catalyst, which decreases the amount of reactive hydroxyl free radicals attacking the BPA molecules and leads to the diminution of BPA photodegradation efficiency [22].

3.2.2 Effects of the initial concentration of H_2O_2

In this section four different initial concentrations of H_2O_2 were tested in the photo-Fenton-like oxidation of BPA over a 1 wt% Fe/TiO_2 catalyst. The selected concentrations of H_2O_2 are 1.5, 2, 3, and 4 times (3.6 mM, 4.7 mM, 7.2 mM, and 9.6 mM) of the stoichiometric ratio according to the equation:

oxidation due to the hydroxyl radical scavenging effect of the H_2O_2 itself, see equations (7) and (8), and Eq. (9) the reaction between the ·OH radicals to form H_2O_2.

$$H_2O_2 + OH\cdot \rightarrow HO_2\cdot + H_2O \quad (7)$$

$$HO_2\cdot + OH\cdot \rightarrow H_2O + O_2 \quad (8)$$

$$OH\cdot + OH\cdot \rightarrow H_2O_2 \quad (9)$$

3.2.3 Effects of the catalyst amount

In order to obtain the optimum Fe/TiO_2 catalyst concentration in the reaction system, the effect of various photocatalyst amounts (0.25 g/ dm^3, 0.5 g/ dm^3, and 1 g/ dm^3) was investigated on the degradation efficiency of

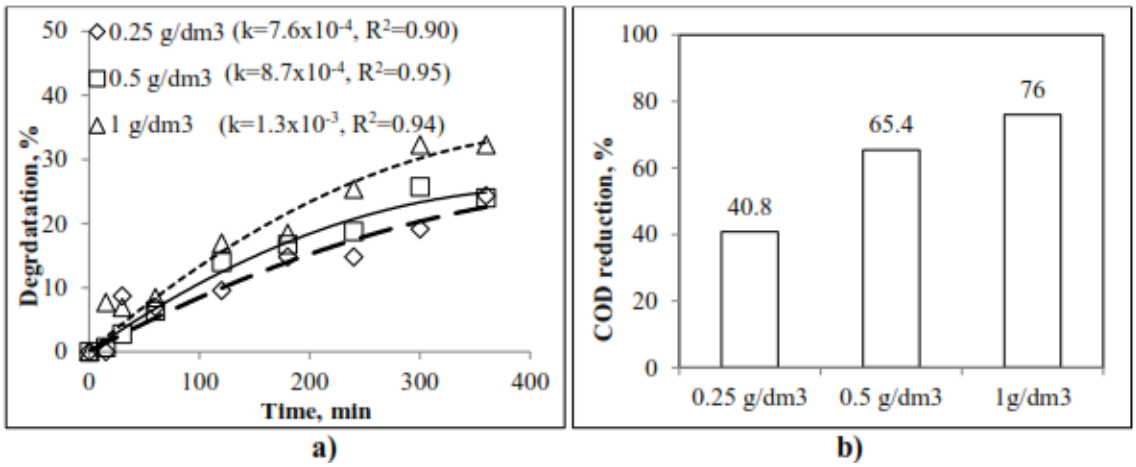

Figure 8. Effects of the catalyst amount on the photo-Fenton-like oxidation, **a)** Degradation, % and **b)** COD reduction, %, after 6 h of oxidation

$$C_{15}H_{16}O_2 + 36\ H_2O_2 \rightarrow 15\ CO_2 + 44\ H_2O \quad (6)$$

The experiments were carried out with a 0.5 g/ dm^3 of 1wt% Fe/TiO_2 catalyst, at a temperature of 20±1°C, at the initial concentration of 15 ppm BPA and with a 0.3 dm^3 BPA solution, and the results are shown in Figure 7.

BPA in water at the initial BPA concentration of 15 ppm, at a pH of 5.5, with a 1 wt% Fe/TiO_2 catalyst, at an H_2O_2 concentration of 4.7 mM, at a temperature of 20±1°C and with a solution volume of 0.3 dm^3.

The results are shown in Figure 8.

An increase in the catalyst amount led to increased degradation and COD reduction. The highest degradation of 32.3% was obtained using a 1 g/dm^3 amount of catalyst after a reaction time of 6 h. The COD reduction increased from 40.8% to 65.4% and then to 76.0% by increasing the catalyst amount from 0.25 g/dm^3 to 0.5 g/ dm^3 and then to 1g/ dm^3, respectively. However, no significant change in the initial degradation rate was observed with the increased amount of catalyst. The efficiency increases with the rise in the number of active sites on the catalyst surface for the photocatalytic reaction which is in parallel with the increasing amount of Fe/TiO_2 [21, 63, 64]. As expected, the first order reaction rate constant increased with the increase in the catalyst amount, see Figure 8a.

3.2.4 Effects of initial pH value of BPA

To investigate the effect of the initial pH value of the BPA solution on the photo-Fenton-like oxidation of BPA, experiments were conducted with 5 different pH values: 2.6, 3.8, 5.5, 8.3, and 9.1. Regulation of the pH was accomplished using an H_2SO_4 or NaOH solution. The results are shown in Figure 9.

the hydroxyl groups and four negative carbon atoms in the phenolic group. These properties determine the initial adsorption of the BPA molecules on the TiO_2 surface. Hence, the acidic conditions for pH < 6.25 favor the initial adsorption of BPA on the positively charged TiO_2 surface. On the contrary, as the pH increases and is higher than 6.25, the TiO_2 surface gradually becomes more negatively charged, which results in the development of greater repulsive forces between the TiO_2 surface and the BPA molecules and thus the obstacle of the initial adsorption of BPA on the TiO_2 surface [56]. In addition, a low pH favors OH· radical generation, and the oxidation potential of the highly oxidative radicals decreases with the increasing pH. The OH· radicals have an oxidation potential of 2.65 - 2.80 V at a pH 3, while only 1.90 V at a pH 7.0 as a weaker oxidant [64].

As seen in Figure 9, the acidic pH was favorable for the degradation of BPA and COD reduction. The highest COD reduction achieved was 70.1% at a pH of 3.8. The remarkable decrease in the reaction rate constant was observed by increasing the solution pH from 3.8 to 5.5.

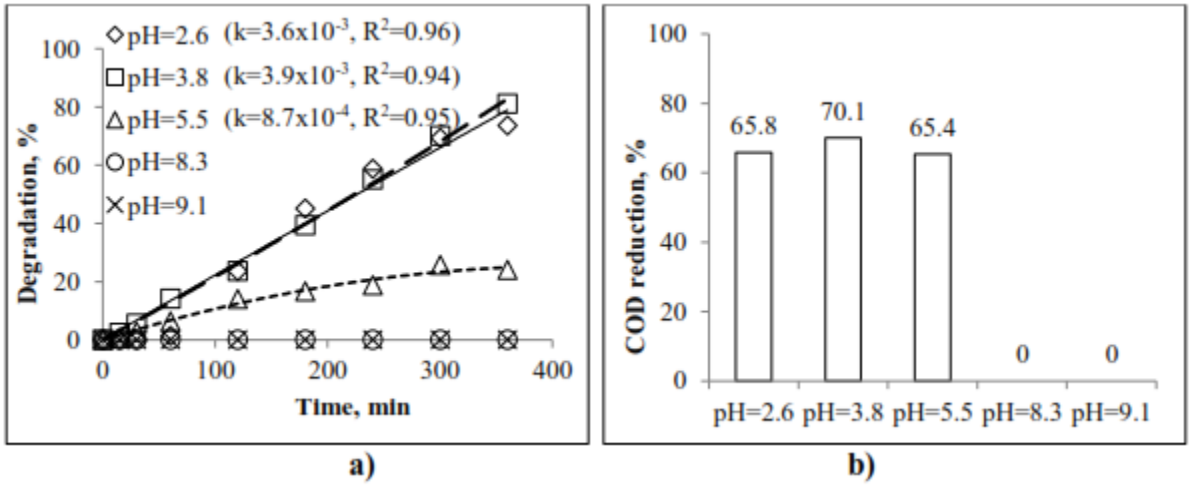

Figure 9. Effects of the BPA initial pH values on the photo-Fenton-like oxidation, **a)** Degradation, % and **b)** COD reduction, %, after 6 h of oxidation

The pH variation can alter the surface property of the catalyst, the ionization state of the organic compound, as well as the formation rate of hydroxyl radicals, and other reactive oxygen species responsible for the pollutant degradation. Therefore, the solution pH is another important factor influencing the BPA photodegradation [62].

In general, the TiO_2 surface is positively charged for pH values lower than the zero point change (zpc) of the TiO_2 (6.25), whereas, it is negatively charged for pH values higher than the zpc of the TiO_2. On the basis of the simulation of the molecular point charge, it was found that the BPA molecule has two negative oxygen atoms in

Adsorption studies in the absence of visible light indicated that a BPA adsorption of 2% was achieved on the catalyst surface in 30 min at a pH of 2.6 and 3.8 while no BPA adsorption was observed at other pH values under the same conditions.

3.2.5 Effects of reaction temperature

The effect of the reaction temperature on the degradation of BPA was examined in the range of 292 - 303K. The experiments were carried out at a pH of 5.5 with a 0.5 g/ dm^3 of 1wt% Fe/TiO_2 catalyst, at an H_2O_2 concentration of 4.7 mM with a 15 ppm / 0.3 dm^3 BPA solution. The results are shown in Figure 10.

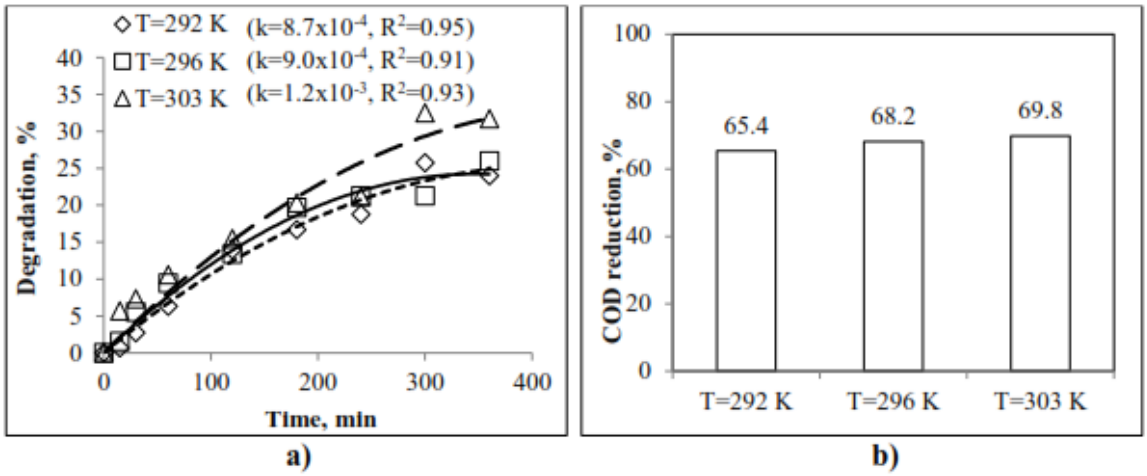

Figure 10. Effects of reaction temperature on the photo-Fenton-like oxidation **a)** Degradation, % and **b)** COD reduction, %, after 6 h of oxidation

As seen in Figure 10, as the temperature increased from 292 K to 303 K, the degradation percentage of BPA increased from 24.0% to 31.7% mainly due to the increase in the rate constant of the heterogeneous photo-Fenton-like reaction, see Figure 10a. Increasing the temperature from 292K to 296K and then to 303K, increased the COD reduction from 65.5% to 68% and to 69.8% after a reaction of 6 h, respectively. The optimum temperature was selected as 303K [14].

3.2.6 Stability of the catalyst

The catalyst stability experiments were carried out under the following conditions: a 15 ppm initial concentration of BPA with a 0.3 dm^3 BPA solution, at a H_2O_2 concentration of 4.7 mM, with a 0.5 g/ dm^3 catalyst, at a pH of 5.5. Firstly the experiment was performed with a fresh catalyst (first cycle). To recover the catalyst, after 6h of reaction, the final effluent was filtered. The used catalyst was washed with water and then ethanol, and then dried at 393K for 3 h and calcined at 773K for 3h. The calcined catalyst was then tested in the photo-Fenton-like degradation of BPA (second cycle). After 6h of reaction the catalyst was recovered as mentioned above and its activity was again tested in BPA oxidation (third cycle). The results are given in Figure 11.

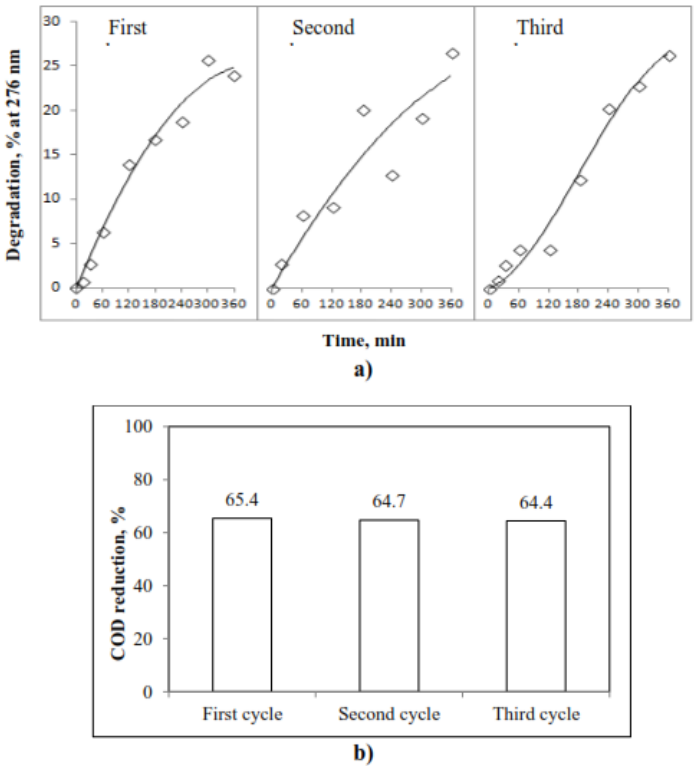

Figure 11. Stability of the Catalyst **a)** Degradation,%, and **b)** COD reduction, %, after 6 h of oxidation

As seen in Figure 11, the degradation of BPA was almost the same the when fresh (first cycle) and used catalysts (second and third cycles) were tested. The COD reduction slightly decreased from 65.4% to 64.7% and then to 64.4% for the second and third cycle, respectively. The calculated first order rate constants were similar $8.7x10^{-4}$, $8.0x10^{-4}$, and $7.0x10^{-4}$ min^{-1} for the 1st (fresh), 2nd and 3rd use of the catalyst, respectively.

The stability of the catalyst was also tested by measuring the iron leaching into the solution by an Atomic Absorption spectrometer (Varian 10 plus). In all runs, iron leaching into the solution remained in the range of 0.09 mg/dm^3 - 0.95 mg/dm^3 which is below E.U. directives (<2 mg/dm^3). These results show that the catalyst has a good stability and the process is mainly the heterogeneous photo-Fenton-like process, instead of the homogenous photo-Fenton-like process.

3.2.7 Optimum conditions of the heterogeneous photo-Fenton-like oxidation of BPA

According to the results obtained from Parts 3.2.2 - 3.2.6; the best experimental conditions for the efficient degradation of BPA by heterogeneous photo-Fenton-like oxidation were determined to be:

The initial concentration of BPA = 5 ppm, H_2O_2 concentration = 3.6 mM, catalyst loading=1 g/ dm^3, at a pH of 3.8, at a temperature of 303 K.

Under these conditions 81.3% of degradation and a COD removal of 89.4% were achieved after 6h of reaction.

3.2.8 Degradation kinetics of BPA

In the photo-Fenton-like oxidation of BPA, the reaction mixture was stirred vigorously at 700 rpm. The effect of external diffusion resistance on the degradation rate was calculated using Hougen's criterion and it was found that $(C_b-C_s)/C_b \approx 1.5x10^{-3} < 0.1$, it indicated that $C_b \approx C_s$. So, the external diffusion resistance could be neglected. The internal diffusion resistance was not significant due to the small size of catalyst particles (60 nm). To calculate the effect of the internal diffusion resistance on the degradation rate, the generalized Thiele modulus based on the reaction rate was determined and found to be $1.3x10^{-7}$ which was smaller than 1/3. Hence the effectiveness factor was assumed to be unity [65].

Figure 12 shows the Arrhenius plot of lnk vs. 1/T obtained using the k values given in Figure 10. From the slope of the Arrhenius plot (R^2=0.92) in Figure 12, -E/R, where R is the universal gas constant (8.314 J/mol K), and the activation energy, E, was calculated to be 22.5 kJ/mol. Finally, the degradation rate of BPA can be expressed by the following equation:

$$-r_{BPA}=8.75e^{-22.5/RT}C_{BPA} \quad (10)$$

In literature, the BPA degradation via the hot persulfate treatment process followed the pseudo-first order kinetics with respect to the BPA concentration. Based on the obtained pseudo first order rate constant at the temperature range of 40 - 70 ^{0}C, the activation energy for BPA oxidation was calculated as 184±12 kJ/mol [66]. The oxidation kinetics of BPA by Mn(VII) was described by a second order rate law, but the order with respect to BPA was first order with an activation energy of 67.8 kJ/mol in the temperature range of 10 - 30 °C [67]. In another study, the degradation BPA by hydrogen peroxide activated with $CuFeO_2$, Cu_2O or Fe_3O_4 followed a pseudo first order reaction in kinetics. The calculated activation energies were 53.7 kJ/mol, 54.3 kJ/mol, and 64.9 kJ/mol at temperatures between 10 to 40 °C for $CuFeO_2$, Cu_2O, or Fe_3O_4, respectively [68]. The degradation of BPA with the Co^+/PMS process followed the pseudo first order kinetic model well at a temperature range of 25 - 45 °C with an activation energy of 57.6 kJ/mol [69]. In the other study, the BPA decomposition in the UV/persulfate process was investigated and the activation energy of 26 kJ/mol was calculated for pseudo first order rate constants at the temperatures between 25 ^{0}C to 50 °C [70]. There were also some studies in literature in which the BPA degradation kinetics were described by a pseudo second order reaction model [71, 72]. In a study by Han et al. [72] the degradation of BPA was investigated by ferrate (IV) oxidation and in that study an activation energy of 35.71 kJ/mol was calculated for the second order reaction kinetics with respect to the BPA concentration. The activation energy

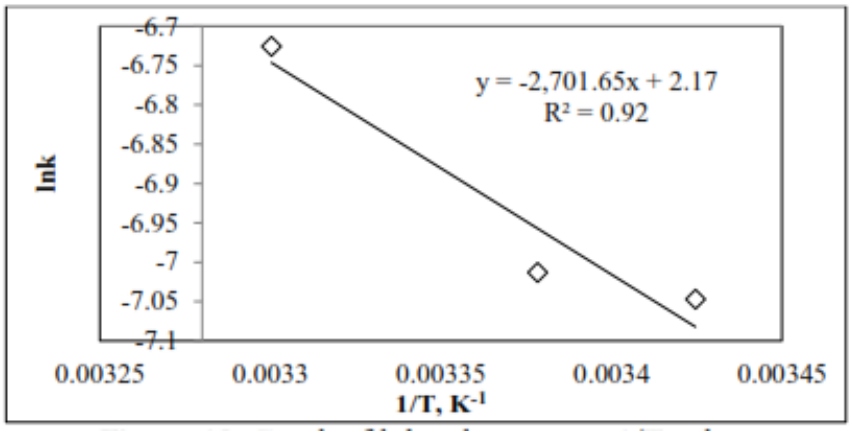

Figure 12. Graph of lnk values versus 1/T values

obtained in this study for the degradation of BPA is close to the one given by Huang and Huang [70].

4. CONCLUSIONS

In the present study, the oxidation of Bisphenol-A was investigated using the heterogeneous photo-Fenton-like oxidation under visible light irradiation in the presence of Fe containing TiO_2 catalyst.

The 1 wt% iron containing TiO_2 catalyst behaves as an efficient and stable catalyst for the photocatalytic degradation of BPA which is an important endocrine disrupting compound. It was clear that the doping of Fe to TiO_2 at a certain amount altered the photocatalytic degradation of BPA under visible light. The photocatalytic activity depended on the Fe loading to the TiO_2, BPA and H_2O_2 initial concentration, catalyst amount, pH of solution, and temperature. At the optimum reaction conditions of, an initial concentration of BPA of 5 ppm, an H_2O_2 concentration of 3.6 mM, a catalyst loading of 1 g/dm^3, a pH of 3.8, and a temperature of 303 K, an 81.3% degradation and a COD removal of 89.4% were achieved after 6h of reaction. The activation energy was calculated to be 22.5 kJ/mol.

ACKNOWLEDGMENTS

The author acknowledges the financial support from the Ege University Scientific Research Fund under project No 13MÜH037. The author also acknowledges the assistance and guidance of Professor Gönül Gündüz during this study.

5. REFERENCES

1. Kang J.H., Kondo F. and Katayama Y., "Human exposure to Bisphenol-A", ***Toxicology***, 226: 79-89, (2006)
2. Er B. and Sarımehmetoğlu B., "Evaluation of presence of Bisphenol-A in foods", ***Vet. Hekim Der***., 82: 69-74, (2011).
3. Zhang K., Gao N., Deng Y., Lin T.F., Ma Y., Li L. and Sui M., "Degradation of Bisphnol-A using ultrasonic irradiation assisted by low-concentration hydrogen peroxide", ***J. Environ. Sci***., 23: 31-36, (2011).
4. Gültekin I. and İnce N.H., "Ultrasonic destruction of Bisphenol-A: The operating parameters", ***Ultrason. Sonochem***., 15: 524-529, (2008).
5. Torres R.A., Petrier C., Combet E., Carrıer M. And Pulgarın C., "Ultrasonic cavitation applied to the treatment of Bisphenol A. Effect of sonochemical parameters and analysis of BPA by-products", ***Ultrason. Sonochem***., 15: 605-611, (2008).
6. Inoue M., Masuda Y., Okada F., Sakurai A., Takahashi I. and Sakakibara, M., "Degradation of Bisphenol A using sonochemical reactions", ***Water Res***., 42: 1379-1386, (2008).
7. Guo Z. and Feng R., "Ultrasonic irradiation-induced degradation of low-concentration Bisphenol A in aqueous solution", ***J. Hazard. Mater***., 163: 855-860, (2009).
8. Petrier C., Torres-Palma R., Combet E., Sarantakos G., Baup S. and Pulgarın, C., "Enhanced sonochemical degradation of Bisphenol-A by biocarbonate ions", ***Ultrason. Sonochem***., 17: 111-115, (2010).
9. Son Y., Lım M., Khım J., Kım L.H. and Ashokkumar, M., "Comparison of calorimetric energy and cavitation energy for the removal of bisphenol-A: The effects of frequency and liquid height", ***Chem. Eng. J***., 183: 39-45 (2012).
10. Torres R.A., Abdelmalek F., Combet E., Petrıer C. and Pulgarin, C., "A Comparative Study of Ultrasonic Cavitation and Fenton's Reagent for Bisphenol A Degradation in Deionized and Natural Waters", ***J. Hazard. Mater***., 146: 546-551, (2007).
11. Ioan I., Wılson S., Lundanes E. And Neculai, A., "Comparison of Fenton and sono-Fenton Bisphenol A degradation", ***J. Hazard. Mater***., 142: 559-563, (2007).
12. Mohapatra D.P., Brar S.K., Tyagı, R.D. and Surampallı R.Y., "Concominant degradation of Bisphenol A during ultrasonication and Fenton oxidation and production of biofertilizer from wastewater sludge", ***Ultrason. Sonochem***., 18: 1018-1027, (2011).
13. Huang R., Fang Z., Yan X. and Cheng, W., "Heterogeneous sono-Fenton catalytic degradation of Bisphenol A by Fe_3O_4 magnetic nanoparticles under neutral condition", ***Chem. Eng. J.,*** 197: 242-249, (2012).
14. Katsumata H., Kawabe S., Kaneco S., Suzuki T. and Ohta, K., "Degradation of Bisphenol A in water by the Photo-Fenton reaction", ***J. Photoch. Photobio. A***., 162: 297-305, (2004).
15. Lin K., Ding J., Wang H., Huang X. and Gan J., "Goethite-Mediated transformation of Bisphenol A", ***Chemosphere***, 89: 789-795, (2012).
16. Zhou D., Wu F., Deng N. and Xıang, W., "Photooxidation of Bisphenol A (BPA) in water in the presence of ferric and carboxylate salts", ***Water Res***., 38: 4107-4116, (2004).
17. Neamtu M. and Frımmel F.H., "Degradation of endocrine disrupting Bisphenol A by 254 nm irradiation in different water matrices and effect on yeast celss", ***Water Res***., 40: 3745-3750, (2006).
18. Ohko Y., Ando I., Chısa N., Tatsuma T., Yamamura T., Nakashıma T., Kubota Y. and Fujıshıma A., "Degradation of Bisphenol A in water by TiO_2 photocatalyst", ***Environ. Sci. Technol***., 35: 2365-2368, (2001).
19. Chiang K., Lım T.M., Tsen L. and Lee, C.C. "Photocatalytic degradation and mineralization of Bisphenol A by TiO_2 and platinized TiO_2", ***Appl Catal A-Gen.,*** 261: 225-237, (2004).
20. Wang G., Wu F., Zhang X., Luo M. and Deng N., "Enhanced TiO_2 photocatalytic degradation of Bisphenol A by β-cyclodextrin in suspended solutions", ***J. Photoch. Photobio. A***., 179: 49-56, (2006).
21. Tsai W.T., Lee M.K. Su T.Y. and Chang Y.M., "Photodegradation of Bisphenol A in a batch TiO_2 suspension reactor". ***J. Hazard. Mater***., 168: 269-275, (2009).
22. Wang R., Ren D., Xıa S., Zhang Y. and Zhao, J., "Photocatalytic degradation of Bisphenol A (BPA) using immobilized TiO_2 and UV illumination in a horizontal circulating bed photocatalytic reactor (HCBPR)", ***J. Hazard. Mater***., 169: 926-932, (2009).
23. Gao B., Lim T.M., Subagio D.P. and Lim T., "Zr-doped TiO_2 for enhanced photocatalytic degradation of Bisphenol A"., ***Appl Catal A-Gen***., 375: 107-115, (2010).

24. Kuo C., Wu C. and Lin H., "Photocatalytic degradation of Bisphenol A in a visible light/TiO_2 system", ***Desalination***, 256: 37-42, (2010).
25. Wan X. and Lim, T., "Solvothermal synthesis of C-N codoped TiO_2 and photocatalytic evaluation for Bisphenol A degradation using a visible-light irradiated LED photoreactor", ***Appl. Catal. B-Environ***., 100: 355-364, (2010).
26. Qing Z., Jınhua L., Hongchong C., Quanpeng C., Baoxue Z., Shuchuan S. and Weımın, C., "Characterization and mechanism of the photoelectrocatalytic oxidation of organic pollutants in a thin-layer reactor", ***Chinese J. Catal.***, 32: 1357-1363, (2011).
27. Yang J., Dai J. and Li, J., "Synthesis, characterization and degradation of Bisphenol A using Pr, N co-doped TiO_2 with highly visible light activity", ***Appl. Surf. Sci.***, 257: 8965-8973, (2011).
28. Li F.B., Lı X.Z., Lıu C.S. and Lıu, T.X., "Effect of alumina on photocatalytic activity of iron oxides for Bisphenol A degradation", ***J. Hazard. Mater***., 149: 199-207, (2007).
29. Wang C., Zhu L., Song C., Shan G. and Chen P., "Characterization of photocatalyst $Bi_{3.84}W_{0.16}O_{6.24}$ and its photodegradation on Bisphenol A under simulated solar light irradiation", ***Appl. Catal. B-Environ***., 105: 229-236, (2011).
30. Wang C., Zhu L., Wei M., Chen P. and Shan, G., "Photolytic reaction mechanism and impacts of coexisting substances on photodegradation of Bisphenol A by Bi_2WO_6 in water", ***Water Res***., 46: 845-853, (2012).
31. Wang C., Zhu L., Chang C., Fu Y. and Chu X., "Preparation of magnetic composite photocatalyst $Bi_2WO_6/CoFe_2O_4$ by two-step hydrothermal methos and its photocatalytic degradation", ***Catal. Commun***., 37: 92-95, (2013).
32. Katsumata H., Taniguchi M., Kaneco S. and Suzuki T., "Photocatalytic degradation of Bisphenol A by Ag_3PO_4 under visible light", ***Catal. Commun***., 34: 30-34, (2013).
33. Yang X., Tian P., Zhang C., Deng Y., Xu J., Gong J. and Han Y., "Au/Carbon as Fenton-like catalysts for oxidative degradation of Bisphenol A", ***Appl. Catal. B-Environ***., 134-135: 145-152, (2013).
34. Irmak S., Erbatur O. and Akgerman, A., "Degradation of 17 β-estradiol and Bisphenol A in aqueous medium by using ozone and ozone/UV techniques", ***J. Hazard. Mater***., B126: 54-62, (2005).
35. Deborde M., Rabouan S., Mazellier P., Duguet J.P. and Legube, B., " Oxidation of Bisphenol A by ozone in aqueous solution", ***Water Res***., 42: 4299-4308, (2008).
36. Garoma T. and Matsumoto S., "Ozonation of aqueous solution containing Bisphenol A: Effect of operational parameters", ***J. Hazard. Mater***., 167: 1185-1191, (2009).
37. Torres-Palma R.A., Nieto J.I., Combet E., Petrıer C. and Pulgarın C., "An innovative ultrasound, Fe^{2+} and TiO_2 photoassisted process for Bisphenol A mineralization", ***Water Res***,. 44: 2245-2252, (2010).
38. Lim M., Son Y., Na S. and Khim, J., "Effect of TiO_2 concentration for sonophotocatalytic degradation of Bisphenol A", ***Proceedings of Symposium on Ultrasonic Electronics***, 31: 103-104, (2010).
39. Poerschmann J.,Trommler, U. and Goreckı, T., "Aromatik intermadiate formation during oxidative degradation of Bisphenol A by homogeneous sub-stoichiometric Fenton reaction", ***Chemosphere***, 7: 975-986, (2010).
40. Leiw M.Y., Guai G.H., Wang X., Tse M.S., Mang N.C. and Tan O.K., "Dark ambient degradation of Bisphenol A and Acid Orange 8 as organic pollutants by perovskite $SrFeO_{3-x}$ metal oxide", ***J. Hazard. Mater***., 260: 1-8, (2013).
41. Xie Y.B. and Li X.Z., "Degradation of Bisphenol A in aqueous solution by H_2O_2- assisted photoelectrocatalytic oxidation", ***J. Hazard. Mater***., B38: 526-533, (2006).
42. Wang X. and Lim T.T., "Effect of hexamethylenetetramine on the visible light photocatalytic activity of C-N codoped TiO_2 for Bisphenol-A degradation: Eveluation of photocatalytic mechanism and solution toxicity", ***Appl Catal A-Gen***., 399: 233-241, (2011).
43. Xing R., Wu L., Fei Z. and Wu, P., "Mesopolymer modified with palladium phthalocyaninesulfonate as a versatile photocatalyst for phenol and Bisphenol A degradation under visible light irradiation", ***J. Environ. Sci***., 25(8): 1687-1695, (2013).
44. Zhang L., Wang W., Sun S., Sun Y., Gao E. and Zhang, Z., "Elimination of BPA endocrine disruptor by magnetic $BiOBr@SiO_2@Fe_3O_4$ photocatalyst", ***Appl. Catal. B-Environ***., 148-149: 164-169, (2014).
45. Wang C., Zhu J., Wu X., Xu H., Song Y., Yan J., Song Y., Ji H., Wang K. and Li, H., "Photocatalytic degradation of Bisphenol A and dye by graphene-oxide/Ag_3PO_4 composite under visible light irradiation", ***Ceram. Int***., 40: 8061-8070, (2014).
46. Sun S., Ding J., Bao J., Gao C., Qi Z., Yang X., He B. and Li C., "Comparison of calorimetric energy and cavitation energy for the removal of Bisphenol-A: The effcets of frequency and liquid height", ***Appl. Suf. Sci***., 258: 5031-5037, (2012).
47. Pelaez M., Nolan N.T., Pillai S.C., Seery M.K., Falaras P,. Kontos A.G,. Dunlop P.S.M., Hamolton J.W.J., Byrne J.A., O'Shea K., Entezari M.H. and Dionysiou D.D., "A review on the visible light active titanium dioxide photocatalysts for environmental applications", ***Appl. Catal. B-Environ***., 125: 331-349, (2012).
48. Lezner M., Grabowska E. and Zaleska A., "Preparation and photocatalytic activity of iron- modified titanium dioxide photocatalyst", ***Physicochem. Probl. Mi***., 48: 193-200, (2012).
49. Akın-Ünnü B., Gündüz G. and Dükkancı M., "Heterogeneous Fenton-like oxidation of Crystal Violet using an iron loaded ZSM-5 zeolite". ***Desalin. Water Treat***., 57: 11835-11849, (2016)
50. Arana J., Diaz G., Saracho M.M., Rodrigez J.M.D., Melian J.A.H. and Pena J.P., "Maleic acid photocatalytic degradation using Fe-TiO_2 catalysts: Dependence of the degradation mechanism on the Fe catalysts content", ***Appl. Catal. B-Environ***., 36(2): 113-124, (2002).
51. Demir N., Gündüz G. and Dükkancı, M., "Degradation of a textile dye, Rhodamine 6G (Rh6G), by heterogeneous sonophotoFenton process in the presence of Fe containing TiO_2 catalysts", ***Environ. Sci. Pollut. R***., 22: 3193-3201, (2015).
52. Khalid N.R., Ahmed E., Ikram M., Ahmed M., Phoenix D.A., Elhissi A., Ahmed W. and Jackson M.S., "Effects of Calcination on Structural Photocatalytic Properties of

TiO_2Nanopowders via $TiCl_4$ Hydrolysis", ***J Mater. Eng. Perform***., 22: 371-375, (2013).

53. Tayade R.J., Surolia P.K., Kulkami R.G. and Jasra, R.V., "Photocatalytic degradation of dyes and organic contaminants in water using nanocrystalline anatase and rutile TiO_2",. ***Sci. Technol. Adv. Mat***., 8: 455-462, (2007).
54. Zhao B.X., Shi B.C., Zhang X.L., Cao X. and Zhang, Y.Z., "Catalytic wet hydrogen peroxide oxidation of H-acid in aqueous solution with TiO_2–CeO_2 and Fe/TiO_2–CeO_2 catalysts", ***Desalination***, 268: 55-59, (2011).
55. Jamalluddin N.A. and Abdullah A.Z., "Reactive dye degradation by combined Fe(III)/TiO_2 catalyst and ultrasonic irradiation: Effect of Fe(III) loading and calcination temperature", ***Ultrason. Sonochem***., 18: 669-678, (2011).
56. Wang A.J., Cuan A., Salmanes J., Nava N., Castillo S., Moranpineda M. and Rojas, F., "Studies of sol-gel TiO_2 and Pt/TiO_2 catalysts for NO reduction by CO in an oxygen reach condition", ***Appl. Surf. Sci***., 230: 94-105, (2004).
57. Seo D.K., Hoffmann R., "Direct and indirect band gap types in one-dimensional conjugated or stacked organic materials", ***Theor Chem Acc***., 102:23-32, (1999).
58. Hörmann U., Kaiser U., Albrecht M., Geserick j., Hüsing N., "Structure and luminescence of sol-gel synthesized anatase nanoparticles", ***16th International Conference on Microscopy of Semiconducting Materials, J. Physics: Conference Series***, 012039, 209:1-6, (2010).
59. Mi J.L., Johnsen S., Clausen C., Hald P., Lock N. So L. and Iversen B.B., "Highly controlled crystallite size and crystallinity of pure and iron-doped anatase-TiO_2 nanocrystals by continuous flow supercritical synthesis", ***J. Mater. Res***., 28: 333-339, (2013).
60. Ganesh I., Kumar P.P., Gupta A.K., Sekhar P.C.S., Radha K., Padmanabham G. and Sundararajan G., "Preparation and characterization of Fe-doped TiO_2 powders for solar light reponse and photocatalytic applications", ***Proc. Appli. Cera***., 6: 21-36, (2012).
61. Akpan U.G. and Hameed B.H., "Parameters affecting the photocatalytic degradation of dyes using TiO_2- based photocatalysts: A review", ***J. Hazard. Mater***., 170: 520-529, (2008).
62. Lu N., Lu Y., Liu F., Zhao K., Yuan X., Zhao Y., Li Y., Qin H. and Zu, J., "$H_3PW_{12}O_{40}$/TiO_2 catalyst-induced photodegradation of Bisphenol A (BPA): Kinetics, toxicity and degradation pathways", ***Chemosphere***, 91: 1266-1272, (2013).
63. Chen Y., Wang K. and Lou L., "Photodegradation of dye pollutants on silica gel supported TiO_2 particles under visible light irradiation", ***J. Photoch. Photobio. A***., 163: 281-287, (2004).
64. Chen A., Ma X. and Sun H., "Decolorzation of KN-R catalyzed by Fe-containing Y and ZSM-5 zeolites", ***J. Hazard. Mater***., 156: 568-575, (2008).
65. Fogler H.S., "Elements of Chemical Reaction Engineering", ***Prentice Hall PTR***, Third Edition, 698 and 703, (1999).
66. Olmez-Hanci T., Alaton I.A. and Genç B., "Bisphenol A treatment by the hot persulfate process: Oxidation products and acute toxicity", ***J. Hazard. Mater***., 261: 283-290, (2013).
67. Zhang J., Sun B. and Guan X., "Oxidative removal of Bisphenol A permanganate: Kinetics, pathways and influences of co-existing chemicals", ***Sep. Purif. Technol***., 107: 48-53, (2013).
68. Zhang X., Ding Y., Tang H., Han X., Zhu L.and Wang N., "Degradation of Bisphenol A by hydrogen peroxide activated with $CuFeO_2$ micoparticles as a heterogeneous Fenton-like catalyst: Efficiency, stability and mechanism", ***Chem. Eng. J***., 236: 251-262, (2014).
69. Huang Y.F. and Huang, Y.H., "Behavioral evidence of the dominant radicals and intermediates involved in bisphenol A degradtion using an efiicient Co^{2+}/PMS oxidation process", ***J. Hazard. Mater***., 167: 418-426, (2009).
70. Huang Y.F. and Huang Y.H., "Identification of produced powerful radials involved in the mineralization of bisphenol A using a novel UV-$Na_2S_2O_8$/H_2O_2-Fe(II,III)", ***J. Hazard. Mater***., 162: 1211-1216, (2009).
71. Zhang P., Zhang G., Dong J., Fan M. and Zeng, G., "Bisphenol A oxidative removal by ferrate (Fe(IV)) under a weak acidic condition", ***Sep. Purif. Technol***., 84: 46-51, (2012).
72. Han Q., Wang H., Dong W., Liu T., Yin Y. and Fan H., "Degradation of bisphenol A by ferrate (IV) oxidation: kinetics, products and toxicity assestment", ***Chem. Eng. J***., 262: 34-40, (2015)